Journal of Food Engineering 397 (2025) 112593

Contents lists available at ScienceDirect

Journal of Food Engineering

journal homepage: www.elsevier.com/locate/jfoodeng

A new chemical marker method for determining heating patterns in microwave pasteurization

Xu Zhou [a,b], Huimin Lin [a], Cheng-You Wu [a], Shyam S. Sablani [a], Juming Tang [a,b,*]

[a] Department of Biological Systems Engineering, Washington State University, Pullman, WA, 99164, USA
[b] Department of Industrial & Systems Engineering, University of Washington, Seattle, WA, 98195, USA

ARTICLE INFO

Keywords:
Gellan gel
Time-temperature indicator (TTI)
Temperature mapping
Chemical marker
Color kinetics

ABSTRACT

Microwave pasteurization provides faster heating and better product quality than conventional thermal pasteurization of pre-packaged foods, but determining microwave heating patterns is a challenge. This study developed a new chemical marker method using a fructose-lysine gellan gel model food to visualize heating patterns in packages. Isothermal heating tests at 70, 80, and 90 °C showed that L^* values of the model food followed first-order reaction kinetics. There was a strong correlation between the L^* values and pasteurization lethality ($F_{90°C}$), suggesting that the changed L^* values in the model food could indicate cumulative time-temperature effects of pasteurization. A color map of the model food was created based on L^* values. The map clearly identified hot and cold spots in the heated model foods, which matched the results from both computer simulations and direct temperature measurements. This study presents a new, cost-effective chemical marker method suitable for rapidly mapping microwave heating patterns in industrial pasteurization processes.

1. Introduction

Microwave heating efficiently transfers energy to food products through plastic packaging, offering potential for rapid in-package sterilization and pasteurization (Tang, 2015; Tang et al., 2018). Identifying cold and hot spots in pre-packaged solid foods is a critical step in developing commercial microwave-based thermal processes. Common temperature measurement methods used in microwave heating, such as fiber optic sensors and infrared imaging, are not suitable, particularly in continuous operations (Wang et al., 2004; Zhou and Tang, 2024).

To overcome this challenge, scientists at the U.S. Army Natick Soldier Center developed a chemical marker method based on Maillard reaction products for sterilization processes (Kim et al., 1994, 1996; Prakash et al., 1997). Three intrinsic markers (M-1, M-2, and M-3) were identified that follow first-order reaction kinetics, which are similar to microbial inactivation (Kim et al., 1996; Lau et al., 2003; Wang et al., 2004). Cumulative heating at different locations in a food package can be determined by measuring the yields of the chemical markers using HPLC (high-performance liquid chromatography). However, HPLC is very time-consuming. According to Pandit et al. (2007a, b), analyzing three layers in a single food tray by two individuals took three days. To improve the procedure, Pandit et al. (2007b) correlated browning color values (on gray scale) with chemical marker yields and sterilization lethality ($F_{121°C}$). This led to the development of a computer vision method for heating patterns based on color changes, reducing analysis time to just a few minutes.

Several model foods containing chemical marker precursors, such as whey protein gel with 1 % ribose (Lau et al., 2003) and mashed potato with 1.5 % ribose (Pandit et al., 2006), were developed for microwave-assisted sterilization at 110–130 °C). However, these model foods are not suitable for pasteurization at lower temperatures (70–90 °C). Whey protein gel requires pre-heating (~80 °C) for gel formation (Lau et al., 2003). This pre-heating can initiate Maillard browning before microwave pasteurization, making it difficult to track color changes resulting from only pasteurization. Mashed potato with 1.5 % ribose had very slow Maillard reaction rates at pasteurization temperatures (Pandit et al., 2006; Jain et al., 2017), limiting the ability to detect subtle color differences.

Pasteurization is defined as “any process, treatment, or comination thereof, that is applied to food to reduce the most resistant microorganism(s) of public health significance to a level that is not likely to present a public health risk under normal conditions of distribution and storage” by National Advisory Committee on Microbiological Criteria for Foods (NACMCF, 2006). A common industrial practice is to achieve a

* Corresponding author. Department of Industrial & Systems Engineering, University of Washington, USA.
E-mail addresses: xuzhou@uw.edu (X. Zhou), jutang88@uw.edu (J. Tang).

https://doi.org/10.1016/j.jfoodeng.2025.112593
Received 6 October 2024; Received in revised form 10 March 2025; Accepted 27 March 2025
Available online 27 March 2025

Table 1
Composition of gellan gel model food formulations[a] with different amounts of fructose, lysine, and ribose (%, w/v).

Formulations	D-fructose	L-lysine	D-ribose
#1	0	0	0
#2	4.0	0	0
#3	2.0	1.0	0
#4	4.0	2.0	0
#5	0	1.0	1.0
#6	0	2.0	2.0

[a] Gellan gum (1.0 %, w/v), $CaCl_2$ (0.1 %, w/v), TiO_2 (0.2 %, w/v), and water (100 mL) were constant for all formulations.

6-$\log_{10}$ reduction of *Listeria monocytogenes* or non-proteolytic *Clostridium botulinum* (ECFF, 2006). For pH-neutral ready-to-eat meals, *Listeria monocytogenes* ($D_{70°C}$ = 0.3 min) is the most heat-resistant vegetative pathogen (ECFF, 2006). It can survive freezing and grow under refrigerated conditions, making it a concern for frozen and chilled food products. To achieve a 6-log reduction of *L. monocytogenes*, heating to 70 °C and held for 2 min or an equivalent process is required. The ready-to-eat meals processed under such conditions have up to 10 days for storage above freezing but at or below 5 °C (Tang et al., 2018). Non-proteolytic *C. botulinum* ($D_{90°C}$ = 1.5 min), a spore-forming bacterium, can grow and produce toxins in low temperature (minimum growth temperature: 3 °C) and low-oxygen environment (ECFF, 2006), which makes it a concern for vacuum or modified atmosphere packaged chilled meals beyond 10-day storage at or above 5 °C. Pasteurization at 90 °C for 10 min or an equivalent process is recommended to achieve a 6-log reduction of non-proteolytic *C. botulinum*. This will give the food products a shelf-life of 6 weeks at < 5 °C (Peng et al., 2017). Both pasteurization processes (70 °C/2 min or 90 °C/10 min) are not able to eliminate more heat-resistant proteolytic *C. botulinum*. Proteolytic *C. botulinum* has a minimum growth temperature of 10–12 °C, minimum pH of 4.6, and a minimum water activity of 0.93 (ECFF, 2006; Zhou and Tang, 2024). Thus, the storage temperature is a critical control factor in distribution chains and at homes to ensure that pasteurized pH-neutral food meals remain safe (Peng et al., 2017).

Microwave-Assisted Pasteurization System (MAPS) developed at Washington State University is designed to produce pH-neutral, vacuum-packaged or nitrogen-flushed ready-to-eat meals, following the guidelines discussed above (Tang et al., 2018; Zhou and Tang, 2024). In developing a pasteurization process schedule, the heating pattern (showing cold and hot spot locations) in the prepackaged food is first determined using a chemical marker method. Mobile temperature sensors then measure the temperatures at the identified cold spots. The belt speed and/or microwave power level are adjusted accordingly to bring the cold spot temperature to above 70 or 90 °C during microwave heating, depending on the targeted patogens and desired shelf-life. The products are then held in hot water until the desired level of pasteurization is achieved. Some model foods have been developed for microwave-assisted pasteurization. Jain et al. (2017) and Wang et al.

Table 2
Dielectric properties of gellan gum model food (formula #4) at 915 MHz used in computer simulation (n = 3).

Temperature (°C)	Dielectric constant	Loss factor
25	81.6 ± 9.9	15.5 ± 1.3
50	72.8 ± 3.1	15.8 ± 1.8
65	69.7 ± 3.2	16.4 ± 2.3
80	66.8 ± 6.0	18.4 ± 2.8
95	67.4 ± 0.1	22.4 ± 1.1

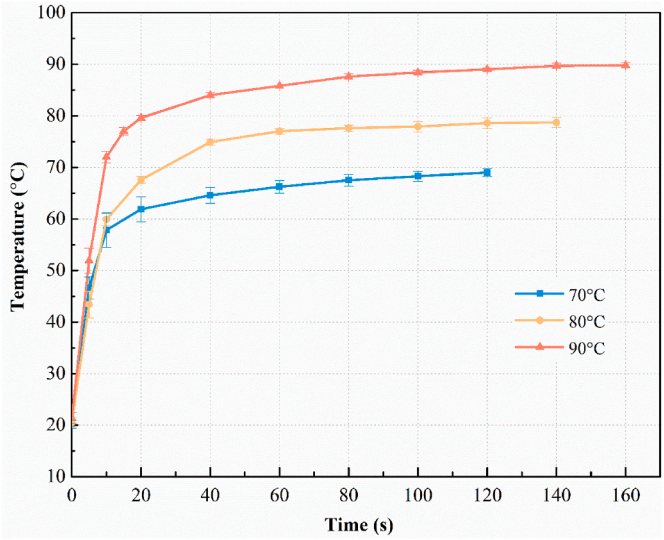

Fig. 2. Heating curves of model food samples in thermal kinetic cells immersed in water baths at 70, 80, and 90 °C, n = 6.

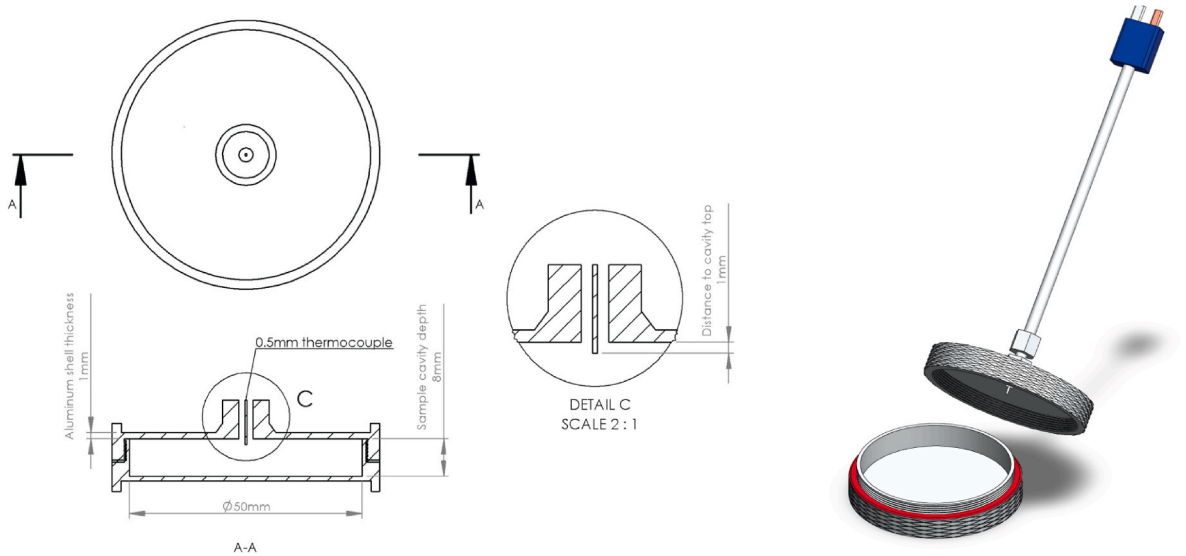

Fig. 1. Thermal kinetic cell.

Table 3
First-order kinetic parameters for L^* color changes of model food samples[a].

Formula	T (°C)	L^*_0	L^*_∞	k ($\times 10^{-3}$ min^{-1})	R^2	E_a (kJ/mol)	R^2	D (min)	z (°C)	R^2
#3[b] (2 %fructose+1 %lysine)	80	74.4	65.6	0.046	0.878	31.4	–	49.8	78.1	–
	90	73.8	54.7	0.062	0.988			37.1		
#4 (4 %fructose+2 %lysine)	70	75.8	65.3	0.036	0.984	50.1	0.956	63.6	47.4	0.962
	80	74.2	50.0	0.050	0.960			46.2		
	90	65.9	43.9	0.096	0.998			24.1		
#5 (1 %ribose+1 %lysine)	70	74.5	66.5	0.022	0.984	74.4	0.992	79.1	32.1	0.994
	80	71.1	55.4	0.054	0.987			42.3		
	90	69.8	52.9	0.123	0.959			18.8		
#6 (2 %ribose+2 %lysine)	70	75.9	57.6	0.053	0.956	176.1	0.900	438.7	13.6	0.889
	80	73.8	44.3	0.080	0.995			28.7		
	90	61.7	38.6	0.154	0.997			14.9		

[a] Formula #1 and #2 were not included due to no significant color change.
[b] Formula #3 at 70 °C was not included due to no significant color change.

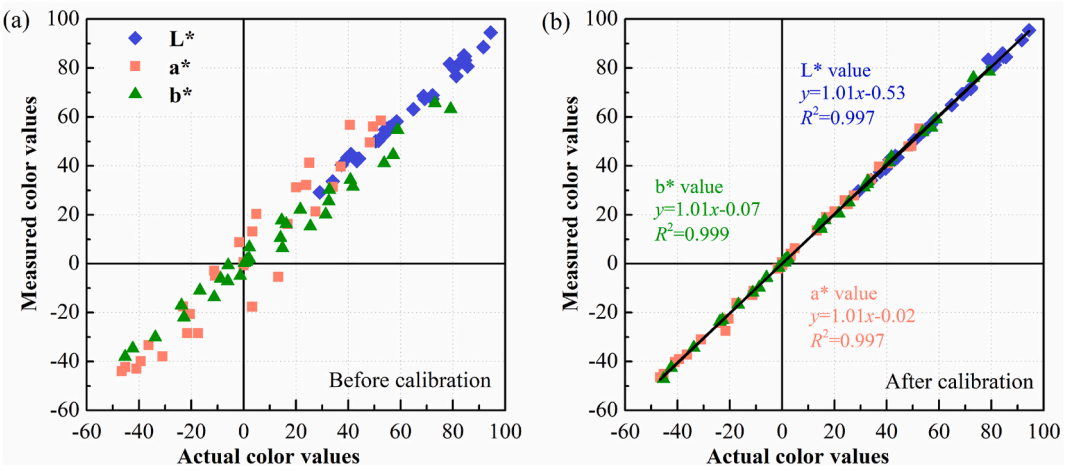

Fig. 3. Comparison of measured color values (L^*, a^*, and b^*) with actual color values of calibration card (known values provided by the manufacturer Argraph Corp., NJ, USA); (a) Before calibration. (b) After calibration. (For interpretation of the references to color in this figure legend, the reader is referred to the Web version of this article.)

(2018) used fructose or ribose caramelization as a chemical marker method, but the reactions required a strongly alkaline environment (pH ~11) to induce browning at pasteurization temperatures. The high pH is impractical for industrial applications. Bornhorst et al. (2017a, c) evaluated Maillard reaction-based model foods, including egg white, mashed potato, and gellan model foods, with a focus on developing model foods for quality evaluation.

We are currently evaluating the performance of solid-state microwave generators in food applications (Zhou et al., 2023a, 2023b) and, in particular, investigating the application of 915 MHz solid-state generators in MAPS. Our preliminary tests using solid-state-powered MAPS revealed a limitation of the existing model foods: they did not produce visible color changes after short microwave heating periods. This highlights the need for a new chemical marker method with greater thermal sensitivity. The new model food should generate stronger and faster color changes to better facilitate the study of solid-state microwave heating and support microwave heating system design. For this reason, we selected ribose-lysine and fructose-lysine as chemical marker precursor systems. Ribose-lysine was chosen based on our previous studies (Bornhorst et al., 2017a, 2017b, 2017c), which showed its effectiveness in producing color changes. We adjusted concentrations to improve sensitivity for short microwave heating. Fructose-lysine was introduced as a cost-effective alternative to ribose-lysine. Therefore, the objectives of this study were to: 1) study color change kinetics of ribose-lysine and fructose-lysine in gellan gum model food, 2) develop a visualization method based on the kinetic result, and 3) validate the method with the pilot-scale solid-state powered MAPS.

2. Materials and methods

2.1. Chemical marker carrier

Model foods serve as carriers for chemical marker precursors. Previous studies (Zhang et al., 2015; Wang et al., 2018) identified low-acyl gellan gum as a suitable carrier with three unique features: 1) low-acyl gellan gum solutions rapidly form gels when cooled to their gelling temperatures and the gels are thermally stable up to 120 °C; 2) these gels are also strong enough to withstand post-processing handling, such as cutting for multilayer analysis; and 3) dielectric properties of the gels can be adjusted to match those of real food products by adding sucrose or salt.

Another reason for selecting gellan gum is that the gelling temperature of gellan solutions can be controlled by adjusting the concentrations of the gellan polymer and charged ions (Tang et al., 1997a, 1997b). Gellan gum powder dissolves in water when heated above 90 °C, breaking into single chains to form a solution. Upon cooling, the gellan chains reassemble into double helices, which are stabilized by cations (e.g., Ca^{2+}, Mg^{2+}). These cations promote cross-linking between the helices, resulting in a three-dimensional gel network and solidification of the gel (Chandrasekaran et al., 1988; Tang et al., 1997a, 1997b). For chemical marker model foods, reducing sugars and amino acids are added to the gellan solution and thoroughly mixed before gelation. As the gel sets, these chemical markers become trapped within the matrix. The gelling temperature of the gellan solutions should be adequately low to avoid chemical marker reactions during gelation. The relationship

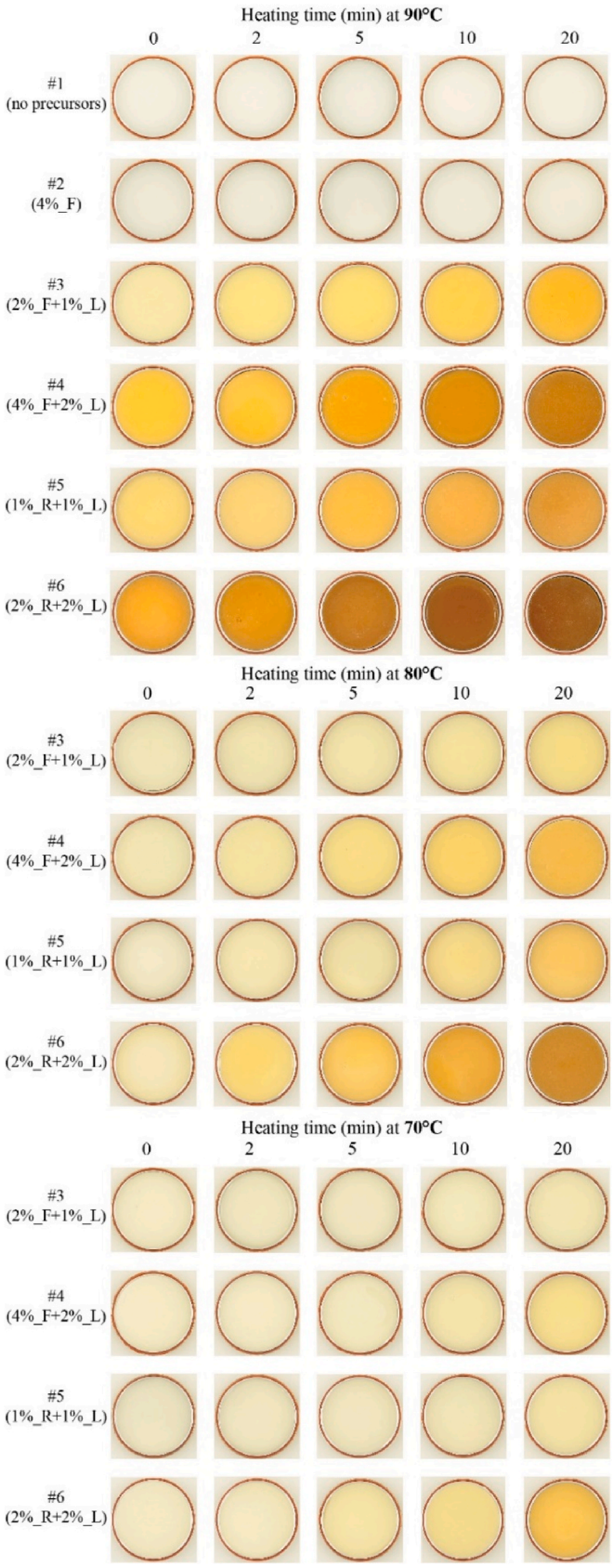

Fig. 4. Surface color of different sample formulas (Table 1) after heating at 70, 80, and 90 °C for 0–20 min (excluding come-up time). (For interpretation of the references to color in this figure legend, the reader is referred to the Web version of this article.)

between the gelling temperature and the concentrations of the gellan polymer and calcium ions was described by Tang et al. (1997b):

$$\frac{1}{T_{gel}} = -5.82 \times 10^{-5} \ln(X_p) - 1.01 \times 10^{-4} \ln(X_i) + 3.33 \times 10^{-3} \quad (1)$$

where T_{gel} is the gelling temperature (absolute temperature in K), X_p is the polymer concentration (g/mL), and X_i is the calcium concentration (mM).

In pasteurization processes at 70–90 °C, an ideal model food should show different levels of color changes within this temperature range to allow identification of heating differences. The gelling temperature, thus, must be below 70 °C, with lower temperatures being more desirable. For this reason, a gellan solution containing 1 % gellan gum and 10 mM Ca^{2+} was developed, with a gelling temperature predicted to be 50 °C using Eq. (1). The gelling temperature was experimentally measured as 47 °C using a visual observation method (Tang et al., 1997b). Although other combinations of polymer and calcium concentrations could achieve similar or even lower gelling temperatures according to Eq. (1), the 1 % gellan gum and 10 mM Ca^{2+} combination was chosen to have desirable gel texture and strength based on the results of Wang et al. (2018).

2.2. Selection of chemical marker precursor concentrations

Table 1 shows the formulations of chemical marker model foods evaluated in this research. Formulas #1 (no precursors) and #2 (fructose only) were used as controls. The fructose-lysine formulations included #3 (2 % fructose + 1 % lysine) and #4 (4 % fructose + 2 % lysine); the 2:1 fructose-to-lysine ratio was chosen based on preliminary results and Ajandouz et al. (2001). The ribose-lysine formulations included #5 (1 % ribose + 1 % lysine) and #6 (2 % ribose + 2 % lysine); the 1:1 ribose-to-lysine ratio was based on Bornhorst et al. (2017a, b).

Low-acyl gellan gels are naturally translucent, allowing light to pass through (Wang et al., 2018). Light scattering in translucent gels can affect the accuracy of measured color values, particularly in areas with uneven texture after heating. This makes it difficult to accurately capture the color development on a surface with a digital imaging system. To overcome this problem, titanium dioxide (TiO_2, a white coloring agent) was added to gellan gels to make them opaque and minimize light scattering. The resulting gels have consistent, uniform pale color.

2.3. Model food preparation

Model food samples were prepared by mixing gellan gum powder (KELCOGEL, CP Kelco, Atlanta, GA) and titanium dioxide (liquid TiO_2, Lorann Oils, Lansing, MI) with distilled and deionized water in a glass beaker. The mixture was stirred and heated on a hot plate (PC-420, Corning, Glendale, AR). The temperature was monitored by a type-T thermocouple (Omega Engineering, Norwalk, CT). The solution was boiled for 5 min to fully hydrate the gellan polymer. To minimize water loss during boiling, the beaker was covered with aluminum foil.

After the hydration, calcium chloride ($CaCl_2 \cdot 2H_2O$, Avantor Performance Materials, LLC, Radnor, PA) was added to the solution, which was then cooled. When the temperature dropped to about 60 °C, chemical marker precursors, D-fructose (Thermo Fisher Scientific Inc., Nazareth, PA, USA), L-lysine (Thermo Fisher Scientific Inc., Nazareth, PA, USA), and D-ribose (Sigma-Aldrich, Saint Louis, MO, USA), were added based on the formulations in Table 1 and mixed for 1–2 min. When the solution reached approximately 55 °C, it was poured into custom-designed test cells (Fig. 1) for kinetic studies or in plastic trays (138 mm × 94 mm × 20 mm) for MAPS processing. The solutions were cooled at room temperature (20–21 °C) to form gels.

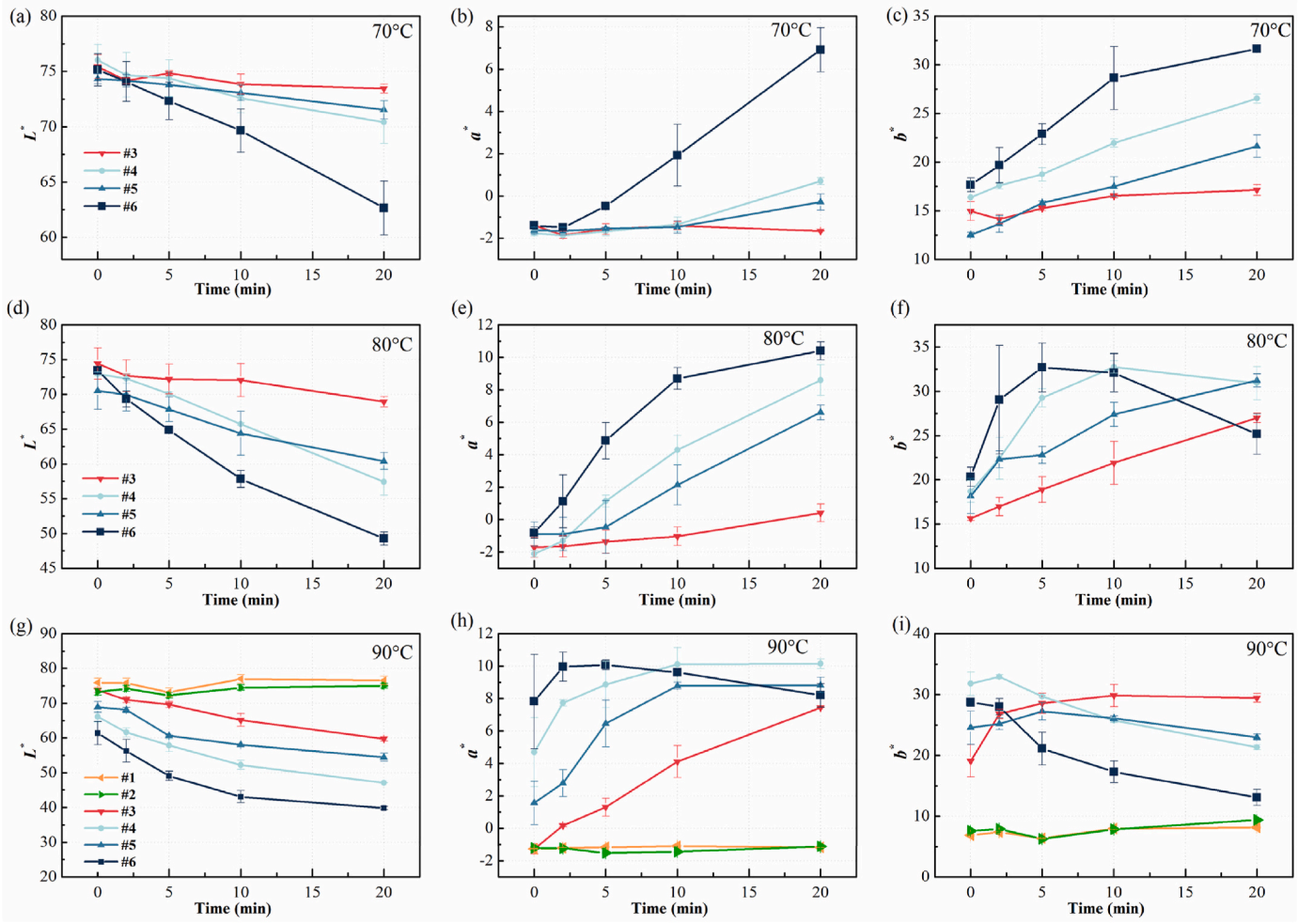

Fig. 5. Color changes of model food samples with different formulations (Table 1) during heating at (a–c) 70 °C, (d–f) 80 °C, and (g–i) 90 °C. At each temperature, (a), (d), and (g) show L^* values; (b), (e), and (h) show a^* values; (c), (f), and (i) show b^* values, $n = 3$. (For interpretation of the references to color in this figure legend, the reader is referred to the Web version of this article.)

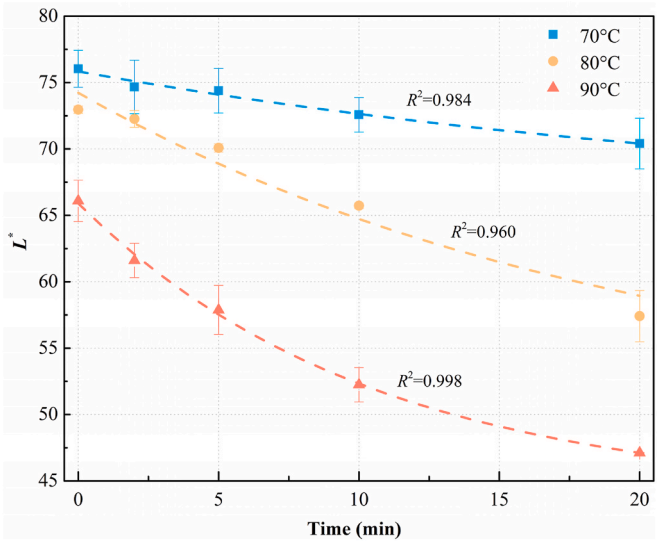

Fig. 6. Changes in L^* values of model food (formula #4) during heating at 70, 80, and 90 °C. Scattered points represent experimental data ($n = 3$) and dashed lines represent first-order kinetic model (Eq. (2)) fits.

2.4. Isothermal kinetic tests

The test cell was made of aluminum, with a diameter of 50 mm, a height of 8 mm, and shell thickness of 1 mm (Fig. 1). When heated in a water or oil bath, this design ensures rapid heat transfer from the circulating liquid to the samples. A type-T thermocouple (0.1 mm diameter) was inserted through the top lid of the cell to monitor the sample temperature.

The test cells containing model food samples (16.2 ± 0.2 g each) were heated in a water bath (2864, Thermo Fisher Scientific, Marietta, OH, USA) at 70, 80, and 90 °C, then cooled in ice water (0 °C). For kinetic studies, the samples were heated for 0, 2, 5, 10, and 20 min excluding the come-up-time (CUT); CUT is the time required for the sample to reach within 1 °C of the set temperature.

2.4.1. Color measurement

The color of the model food samples was measured in CIELAB (L^*, a^*, b^*) values using a computer vision system (Pandit et al., 2007a). The camera settings were based on Bornhorst et al. (2017a), with an aperture (F) of 11, a frame rate of 15 fps, an ISO sensitivity of 200 under D65 daylight illumination conditions. Calibration was performed using QP Card 203 (Argraph Corp., Fairfield, NJ, USA) with 35 standardized color references.

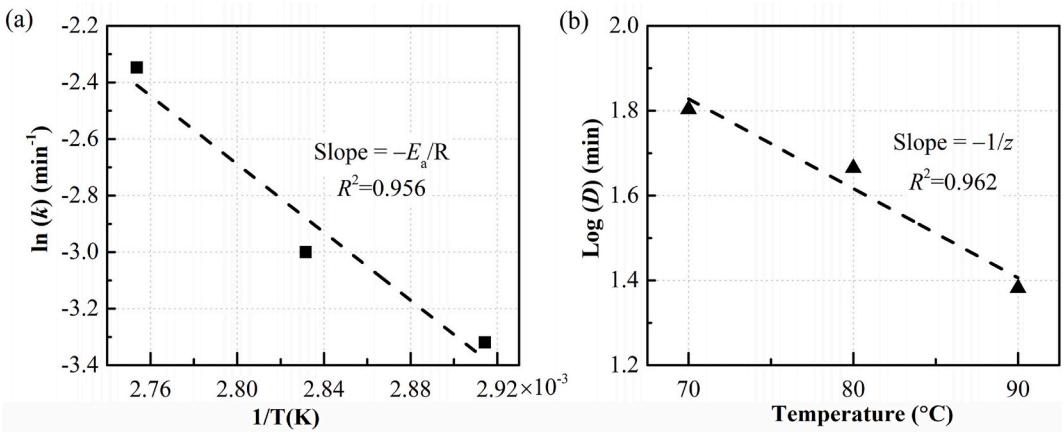

Fig. 7. (a) Arrhenius plot of ln (k) vs. 1/T, used to determine E_a, (b) log (D) vs. T, used to determine z-value.

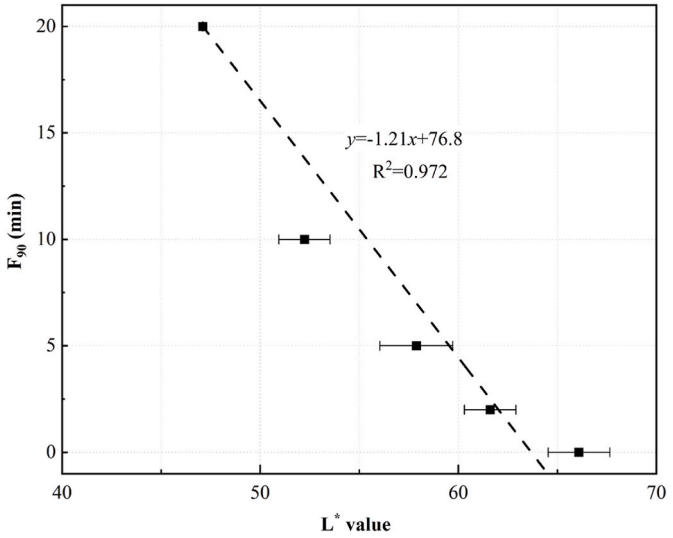

Fig. 8. $F_{90°C}$ correlated with L^* values during 20 min heating at 90 °C for formula #4 model food.

2.4.2. Kinetic models

Previous studies (Bornhorst et al., 2017a, 2017b; Jain et al., 2017; Wang et al., 2018) showed that the color changes during non-enzymatic browning were best described by the modified first-order model:

$$\ln\left(\frac{C-C_\infty}{C_0-C_\infty}\right)=k\bullet t \tag{2}$$

where C is the color value, C_0 is the initial color value, and C_∞ is the maximum or equilibrium color value, t is the heating time (s), and k is the reaction rate constant (1/s).

The reaction rate constant (k) depends on temperature, following the Arrhenius equation:

$$k=k_0\bullet e^{-\frac{E_a}{R\bullet T}} \tag{3}$$

or in logarithmic form:

$$\ln(k)=\ln(k_0)+\left(-\frac{E_a}{R}\right)\bullet\frac{1}{T} \tag{4}$$

where k_0 is the pre-exponential factor (indicative of the rate constant as temperature approaches infinity), E_a is the activation energy (kJ/mol), R is the universal gas constant (8.314 J/K·mol), and T is the absolute temperature (K). The activation energy E_a was graphically determined by plotting ln(k) versus 1/T, as shown in Fig. 7.

Another approach to quantify first-order reactions uses D-value and z-value (Tang et al., 2000). The D-value (min) is the time required for a one-log reduction (90 %) of the color value at a fixed temperature. The z-value (°C) is the temperature change needed for a one-log change in D-values. The D-value at each temperature was determined by plotting the logarithm of color values versus time. The z-value was obtained by plotting the logarithm of D-values versus temperature (Fig. 7).

The accumulated thermal lethality ($F_{90°C}$) during pasteurization was calculated using:

$$F_{90°C}=\int_0^t 10^{(T-90)/z}dt \tag{5}$$

where $F_{90°C}$ is the equivalent thermal treatment time (min) at 90 °C, T is the temperature (°C), t is the time (min), and a z-value of 10 °C was used for nonproteolytic *C. botulinum* (ECFF, 2006).

2.5. Validation in microwave assisted pasteurization

Validation tests were conducted using a pilot-scale 915 MHz single-mode Microwave-Assisted Pasteurization System (MAPS) at Washington State University, Pullman, WA, USA (Zhou and Tang, 2024). The system includes four sections: (1) preheating, (2) microwave heating, (3) holding, and (4) cooling. A detailed description of the system is provided by Tang et al. (2018), with the modification that one magnetron generator was replaced by a 6 kW, 915 MHz solid-state microwave generator (RFHIC Corp., Anyang, South Korea) with two launching heads. For this study, only the solid-state-powered microwave cavity (the 2nd cavity) was active, while the other three cavities operated without microwave power.

During the tests, the trays with model food samples were preheated in 51 °C water for 30 min. The trays were heated in the solid-state-powered microwave cavity at 2 kW with a phase difference of 0° for 2.5 min, held at 91 °C in hot water for 2.5 min, and cooled in 20 °C water for 15 min. After processing, the samples were horizontally sliced in the middle, and the heating patterns in the middle layer were analyzed using Photoshop and MATLAB (2021a, The MathWorks, Inc., Natick, MA, USA).

2.6. Computer simulation

A computer simulation model was developed using COMSOL Multiphysics® (COMSOL Inc., Burlington, MA, USA) to solve Maxwell's and transient heat conduction equations. Boundary conditions, such as perfect electric conductors of metal cavities and convective heat transfer between water and food packages were detailed in previous studies

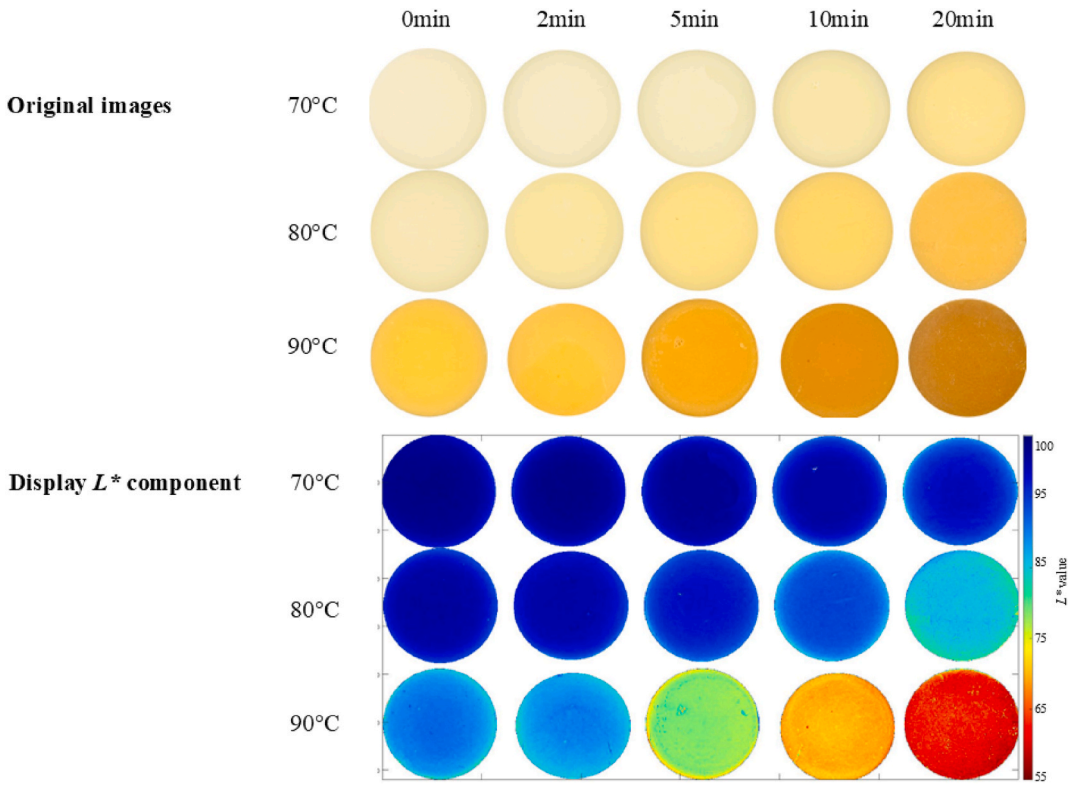

Fig. 9. Original images (top) and L^* map (bottom) of model food (formula #4) during heating at 70, 80, and 90 °C. The L^* components were extracted from the original images.

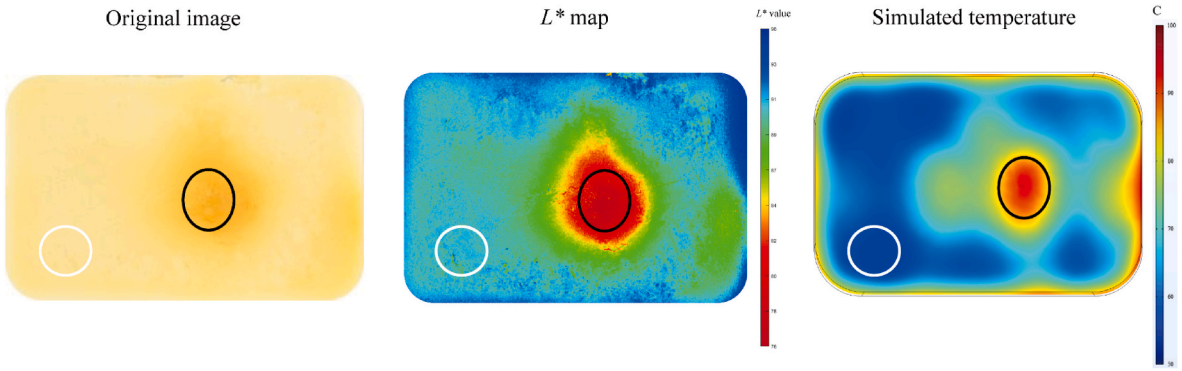

Fig. 10. Original image, L^* based color map, and simulated temperature distribution (°C) of the middle layer of the model food (formula #4) processed in the solid-state powered microwave-assisted pasteurization system (MAPS); black circles: hot spots, and white circles: cold spots. (For interpretation of the references to color in this figure legend, the reader is referred to the Web version of this article.)

(Jain et al., 2018).

The dielectric properties of the model food gels were measured using a network analyzer (E5071C, Keysight Technologies, Inc., Santa Clara, CA, USA) with an open-ended coaxial probe (85070E, Keysight Technologies, Inc., Santa Clara, CA, USA) following the standard calibration procedure described in Zhang et al. (2015) and Zhou et al. (2024). Calibration involved air, distilled water (25 °C), and a shorting block. Table 2 shows the measured dielectric properties at 915 MHz. Thermal properties, including specific heat capacity (C_p, J/kg·°C), density (ρ, kg/m^3), and thermal conductivity (k, W/m·°C) were measured using a Thermal Properties Analyzer (KD2 pro, Decagon Devices, Pullman, WA, USA) with a dual-needle probe (SH-1). The SH-1 probe was calibrated with reference material (DB11-4, Decagon Devices, Pullman, WA, USA) with known thermal property values. The measured values of $\rho \cdot C_p$ (3.7 $\times$ 10^6 J/m^3·°C) and k (0.6 W/m·°C) of the gellan gel were used in the computer simulation.

2.7. Statistical analysis

All experiments were conducted in three replicates, and the results are presented as mean values with 95 % confidence intervals. Statistical analysis was performed using Excel (Microsoft, Redmond, WA) and SAS software (University Edition, SAS Institute Inc., Cary, NC).

3. Results and discussions

3.1. Come-up time

Fig. 2 shows the heating curves of the model food samples in the water bath. The come-up times ranged from 2.0 to 2.7 min, depending

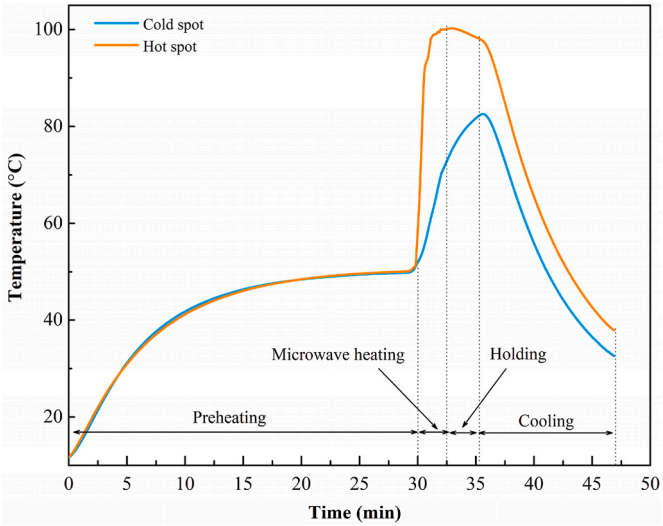

Fig. 11. Temperature profiles at the cold and hot spots (as circled in Fig. 10) in 10.5 oz model food (formula #4) processed in the pilot-scale microwave assisted pasteurization system (MAPS).

on water temperature. These come-up times were much shorter than the *D*-values of color changes in the model foods (15–440 min, Table 3), which means that no significant color changes should happen during the come-up time. To ensure accurate isothermal kinetic studies, however, color values measured immediately after the come-up time were used as the starting points (0-min mark) for the kinetic analysis.

3.2. Color measurement calibration

Color calibration is important for color measurements but is often overlooked. This section highlights the role of calibration in achieving accurate results. Fig. 3 compares the color values measured from the reference cards with the manufacturer-provided values (Argraph Corp., NJ, USA). For the calibration, reference cards were photographed under the same lighting conditions used in the experiments, and QP Calibration software (Argraph Corp., Fairfield, NJ, USA) was used to compare the captured colors with the manufacturer's known values. Image settings, including white balance, exposure, and contrast, were adjusted to minimize differences between the measured and the reference color values. The adjustments were saved as a calibration profile in Photoshop and applied to all experimental images. Fig. 3 shows that before calibration, the measured color values significantly deviated from the reference values, with RMSE ranging from 2.1 to 6.5 and R^2 of 0.988. After calibration, the RMSE values were reduced to below 1.5 and R^2 exceeded 0.997.

3.3. Color map of model foods

Fig. 4 shows the color changes of the model food samples with different chemical marker precursors. The control samples—formula #1 (without precursors) and formula #2 (with only fructose)—showed no significant browning. That means that gellan gum and its base ingredients do not contribute to the Maillard reaction, and that both reducing sugars and amino acids are needed for color changes. Higher precursor concentrations and higher temperatures resulted in more browning.

Comparing the fructose-lysine systems (formulas #3 and #4) with the ribose-lysine systems (formulas #5 and #6) suggested that the ribose-lysine caused more browning. Ribose reacts faster in Maillard reactions than fructose because of its aldehyde group, which facilitates the formation of Schiff bases and Amadori rearrangement products (Ashoor and Zent, 1984; Damodaran et al., 2007). Increasing the fructose concentration to 4 % in formula #4 resulted in browning similar to 2 % ribose in formula #6. That means doubling fructose levels can achieve browning nearly comparable to ribose. Ribose (e.g., $2000 per kg from Sigma-Aldrich, USA, purchased time 2024) costs about 40 times more than fructose (e.g., $50 per kg from Fisher Science Education, USA, 2024), so using fructose is a more cost-effective option for the food industry where large quantities of model foods are required for test runs in developing a microwave-based thermal process.

3.4. CIE LAB color of model foods

Fig. 5 shows that the CIE LAB color changes in the model food samples. L^* values (brightness) decreased over time, with a greater decrease at higher temperatures (Fig. 5a, d, g). The a^* values (green to red) generally increased for all formulas, but for formula #6 at 90 °C, the a^* values initially increased and then declined after extended heating (Fig. 5h). The b^* values (yellow to blue) showed more complicated trends. At 70 °C and 80 °C, b^* values increased over time for most formulas, except for formula #6. At 90 °C, formulas #4, #5, and #6 showed decreasing b^* values (Fig. 5i). The trends in b^* values likely reflect different stages of the Maillard reaction. Initially, yellow-brown compounds were formed, increasing b^* values. At higher temperatures and longer heating times, these compounds reacted further to form darker, less yellow melanoidins (Echavarría et al., 2012). Similar trends were observed by Bornhorst et al. (2017a, b). The a^* and b^* values were excluded from further kinetic analyses due to the weak correlations. The L^* values were used for kinetic studies.

3.5. Kinetic analysis and correlation between color and lethality

Table 3 shows the first-order kinetic parameters for L^* values in model foods. Most formulas were in good agreement with first-order kinetics, with R^2 values greater than 0.95, except for formula #3. The deviations for formula #3 were likely due to a slower Maillard reaction or insufficient heating time. Fig. 6 shows the fitted first-order curves for formula #4 (the most cost-effective option), which demonstrated a strong model fit ($R^2 > 0.96$).

The reaction rate constant (k) increased with higher precursor concentrations and temperatures. Increasing temperature also resulted in lower *D*-values (Table 3 and Fig. 7), following the Arrhenius relationship (Eq. (3)). Ribose-lysine systems exhibited higher k values than fructose-lysine systems at the same temperature, indicating faster reaction rates in the ribose-lysine systems. The activation energies (E_a) and z-values were different for different formulas, reflecting different sensitivities to temperature. A lower z-value corresponds to a higher activation energy E_a, as shown in Eq. (6) (Tang et al., 2000):

$$z = \frac{2.303 \bullet R \bullet T_1 \bullet T_2}{E_a} \tag{6}$$

where T_1 and T_2 are the minimum and maximum absolute temperatures within the test range. Food systems with lower z-values (higher E_a) are more sensitive to temperature changes, and the reaction rate k increases more rapidly with rising temperature. The ribose-lysine systems (formulas #5 and #6) had smaller z-values, ranging from 13 to 32 °C, compared to the fructose-lysine systems (formulas #3 and #4), which had z-values ranging from 47 to 78 °C. That means ribose-lysine model foods are more temperature-sensitive. The z-values for ribose-lysine gellan gum model foods in this study (13.6–32.1 °C) differed slightly from those reported for ribose-lysine mashed potato model foods (20–28 °C, Bornhorst et al., 2017b). The difference was likely due to variations in the food matrix and the addition of titanium dioxide in this study.

Fig. 8 shows that $F_{90°C}$ values (calculated using Eq. (5)) are negatively correlated with L^* values of the model food #4 ($R^2 = 0.972$), suggesting that the L^* values can be used to assess pasteurization safety. The negative correlation suggests that areas with lower L^* values

(darker colors) received more heat, while areas with higher L^* values received less heat.

3.6. A visualization method for heating patterns based on L^* values

The L^* values were extracted from CIELAB color space to create L^* color maps (Fig. 9). While the highest and lowest values of L^* can be used directly to locate the cold and hot spots, respectively, in the model foods, it is desirable to visualize the corresponding overall heating patterns. To improve the interpretation of spatial variations in L^* values, the jet colormap was used to translate L^* values into a spectrum of colors. The jet colormap is a widely used color mapping scheme in scientific visualization (MATLAB, 2024) that assigns colors across the visible spectrum to numerical values. The transformation from L^* values to the jet colormap involved normalizing the L^* values:

$$L_{normalized} = \frac{L^* - L^*_{min}}{L^*_{max} - L^*_{min}} \tag{7}$$

where L^* is the original value, L^*_{min} and L^*_{max} are the minimum and maximum L^* values in the image. After normalization, the $L_{\text{normalized}}$ values were mapped to the corresponding colors in the MATLAB jet colormap. In the jet colormap, blue represents the highest L^* values (the least heating), while red represents the lowest L^* values (the most heating). The color transition follows predefined intervals: blue: $L_{\text{normalized}} = 1$, cyan: $L_{\text{normalized}} = 0.75$, green: $L_{\text{normalized}} = 0.5$, yellow: $L_{\text{normalized}} = 0.25$, Red: $L_{\text{normalized}} = 0$). Fig. 9 shows that the L^* based color maps effectively visualized and highlighted differences across different temperatures and heating times in the test cells.

An interesting question arises: Can L^* values (lightness) alone be used to determine heating patterns of foods processed in microwave pasteurization? To answer this question, the L^* based method was tested using the pilot-scale MAPS.

3.7. Heating pattern validation in microwave pasteurization

Fig. 10 illustrates the original image and L^* based color map of the model food processed by MAPS. The original image showed visible color differences, where the darker regions indicated more intense heating while the lighter regions indicated less heating. This allows easy assessment of microwave heating uniformity between processing runs, even without imaging instruments. The L^* map further enhanced clarity in identifying hot spot and cold spots. To validate the spots, the color map was compared with computer simulations and direct temperature measurements. The spatial pattern of the L^* values agreed with the simulated temperature distribution. Ellab mobile temperature sensors were placed at the identified spots, as suggested by Luan et al. (2015). The L map also closely matched the sensor measurements (Fig. 11).

In earlier work, Pandit et al. (2007a, b) developed a computer vision method to determine heating patterns in model foods for microwave-assisted thermal sterilization. The method involved several steps: converting browning into a grayscale ranging from 0 (unheated) to 255 (maximum browning) and mapping gray values onto a custom rainbow color palette based on thermal lethality ($F_{121^\circ C}$). The images were divided into grids, and gray-level values were extracted using custom scripts in IMAQ Vision Builder (Pandit et al., 2007b). In contrast, the L^* color map method developed in this study is much simplified. It uses MATLAB built-in functions, such as rgb2lab and lab(:,:,1), to create the L^* color map in 1–2 seconds. The MATLAB code is provided in the Appendix.

4. Conclusion

A new chemical marker method was developed to determine heating patterns in microwave-assisted pasteurization processes. The L^* values (brightness) of gellan gum model foods containing fructose-lysine and ribose-lysine precursors followed first-order reaction kinetics. Ribose-lysine systems showed faster color change rates at the same concentration; however, doubling the fructose concentration in fructose-lysine systems achieved comparable browning effects. This provides a cost-effective alternative since fructose is significantly less expensive and more readily available than ribose. The spatial pattern of L^* values in the fructose-lysine model food samples matched closely with the computer simulation and direct temperature measurements. The fructose-lysine gellan gum model food is suited for industrial uses where hundreds of model food packages are needed for each test run.

This study addresses the need for heat-sensitive and cost-effective chemical marker model foods, as well as a simplified method to visualize heating patterns in short-time microwave heating. We will use this tool to study solid-state microwave heating. The tool will also help optimize microwave system design and industrial processing developments.

CRediT authorship contribution statement

Xu Zhou: Writing – original draft, Methodology, Investigation, Formal analysis, Conceptualization. **Huimin Lin:** Methodology, Investigation. **Cheng-You Wu:** Investigation. **Shyam S. Sablani:** Writing – review & editing. **Juming Tang:** Writing – review & editing, Supervision, Conceptualization.

Declaration of competing interest

To the best of our knowledge, the named authors have no conflict of interest, financial or otherwise.

Acknowledgement

The authors acknowledge the financial support provided by the USDA, NIFA AFRI Grant (2023-67017-39831).

Appendix

MATLAB code to generate L* map

```
% Read the RGB image
I = imread('Mid.jpg'); % Replace 'Mid.jpg' with your actual image file

% Convert the RGB image to CIELAB color space
labImage = rgb2lab(I);

% Extract the L* component (lightness)
L = labImage(:,:,1);

% Set the minimum and maximum L* values for visualization
L_min = 50; % Minimum L* value
L_max = 100; % Maximum L* value

% Display L* map
figure;
imagesc(L, [L_min L_max]); % Display L* values with the real range
axis image off; % Remove axis and its labels
colormap(flipud(jet)); % Invert 'jet' colormap so that blue is for high
values, red for low
colorbar; % Add a colorbar to visualize the real L* values
caxis([L_min L_max]); % Ensure color axis reflects the real L* range
title('L* Map');
```

Data availability

Data will be made available on request.

References

Ajandouz, E., Tchiakpe, L., Ore, F.D., Benajiba, A., Puigserver, A., 2001. Effects of pH on caramelization and Maillard reaction kinetics in fructose-lysine model systems. J. Food Sci. 66 (7), 926–931.

Ashoor, S., Zent, J., 1984. Maillard browning of common amino acids and sugars. J. Food Sci. 49 (4), 1206–1207.

Bornhorst, E.R., Tang, J., Sablani, S.S., Barbosa-Cánovas, G.V., 2017a. Development of model food systems for thermal pasteurization applications based on Maillard reaction products. Lebensm. Wiss. Technol. 75, 417–424.

Bornhorst, E.R., Tang, J., Sablani, S.S., Barbosa-Cánovas, G.V., 2017b. Thermal pasteurization process evaluation using mashed potato model food with Maillard reaction products. Lebensm. Wiss. Technol. 82, 454–463.

Bornhorst, E.R., Tang, J., Sablani, S.S., Barbosa-Cánovas, G.V., Liu, F., 2017c. Green pea and garlic puree model food development for thermal pasteurization process quality evaluation. J. Food Sci. 82 (7), 1631–1639.

Chandrasekaran, R., Millane, R.P., Arnott, S., Atkins, E.D., 1988. The crystal structure of gellan. Carbohydr. Res. 175 (1), 1–15.

Damodaran, S., Parkin, K.L., Fennema, O.R., 2007. Fennema's Food Chemistry. CRC press.

ECFF, 2006. European chilled food federation. Recommendations for the Production of Prepackaged Chilled Food. https://www.ecff.eu/publications/. Accessed August 2024.

Echavarría, A.P., Pagán, J., Ibarz, A., 2012. Melanoidins formed by Maillard reaction in food and their biological activity. Food Eng. Rev. 4, 203–223.

Jain, D., Wang, J., Liu, F., Tang, J., Bohnet, S., 2017. Application of non-enzymatic browning of fructose for heating pattern determination in microwave assisted thermal pasteurization system. J. Food Eng. 210, 27–34.

Jain, D., Tang, J., Liu, F., Tang, Z., Pedrow, P.D., 2018. Computational evaluation of food carrier designs to improve heating uniformity in microwave assisted thermal pasteurization. Innov. Food Sci. Emerg. Technol. 48, 274–286.

Kim, H.-J., Ball, D., Giles, J., White, F., 1994. Analysis of thermally produced compounds in foods by thermospray liquid chromatography-mass spectrometry and gas chromatography-mass spectrometry. J. Agric. Food Chem. 42 (12), 2812–2816.

Kim, H.-J., Taub, I.A., Choi, Y.-M., Prakash, A., 1996. Principles and applications of chemical markers of sterility in high-temperature-short-time processing of particulate foods. ACS Symposium Series. American Chemical Society, Washington, DC.

Lau, M., Tang, J., Taub, I., Yang, T., Edwards, C., Mao, R., 2003. Kinetics of chemical marker formation in whey protein gels for studying microwave sterilization. J. Food Eng. 60 (4), 397–405.

Luan, D., Tang, J., Pedrow, P.D., Liu, F., Tang, Z., 2015. Performance of mobile metallic temperature sensors in high power microwave heating systems. J. Food Eng. 149, 114–122.

MATLAB, 2024. Jet colormap array. https://www.mathworks.com/help/matlab/ref/jet.html.

NACMCF, 2006. National Advisory Committee on Microbiological Criteria for Foods. Requisite scientific parameters for establishing the equivalence of alternative methods of pasteurization. J. Food Protect. 69 (5), 1190–1216.

Pandit, R., Tang, J., Liu, F., Mikhaylenko, G., 2007a. A computer vision method to locate cold spots in foods in microwave sterilization processes. Pattern Recogn. 40 (12), 3667–3676.

Pandit, R., Tang, J., Liu, F., Pitts, M., 2007b. Development of a novel approach to determine heating pattern using computer vision and chemical marker (M-2) yield. J. Food Eng. 78 (2), 522–528.

Pandit, R., Tang, J., Mikhaylenko, G., Liu, F., 2006. Kinetics of chemical marker M-2 formation in mashed potato—a tool to locate cold spots under microwave sterilization. J. Food Eng. 76 (3), 353–361.

Peng, J., Tang, J., Barrett, D.M., Sablani, S., Anderson, N., Powers, J.R., 2017. Thermal pasteurization of ready-to-eat foods and vegetables: critical factors for process design and effects on quality. Crit. Rev. Food Sci. Nutr. 57 (14), 2970–2995.

Prakash, A., Kim, H.-J., Taub, I., 1997. Assessment of microwave sterilization of foods using intrinsic chemical markers. J. Microw. Power Electromagn. Energy 32 (1), 50–57.

Tang, J., Tung, M., Zeng, Y., 1997a. Gelling properties of gellan solutions containing monovalent and divalent cations. J. Food Sci. 62 (4), 688–712.

Tang, J., Tung, M., Zeng, Y., 1997b. Gelling temperature of gellan solutions containing calcium ions. J. Food Sci. 62 (2), 276–280.

Tang, J., Ikediala, J.N., Wang, S., Hansen, J.D., Cavalieri, R.P., 2000. High-temperature-short-time thermal quarantine methods. Postharvest Biol. Technol. 21 (1), 129–145.

Tang, J., 2015. Unlocking potentials of microwaves for food safety and quality. J. Food Sci. 80 (8), E1776–E1793.

Tang, J., Hong, Y.K., Inanoglu, S., Liu, F., 2018. Microwave pasteurization for ready-to-eat meals. Curr. Opin. Food Sci. 23, 133–141.

Wang, Y., Lau, M.H., Tang, J., Mao, R., 2004. Kinetics of chemical marker M-1 formation in whey protein gels for developing sterilization processes based on dielectric heating. J. Food Eng. 64 (1), 111–118.

Wang, J., Tang, J., Liu, F., Bohnet, S., 2018. A new chemical marker-model food system for heating pattern determination of microwave-assisted pasteurization processes. Food Bioprocess Technol. 11, 1274–1285.
Zhang, W., Luan, D., Tang, J., Sablani, S., Rasco, Lin, H., Liu, F., 2015. Dielectric properties and other physical properties of low-acyl gellan gel as relevant to microwave assisted pasteurization process. J. Food Eng. 149, 195–203.
Zhou, X., Tang, Z., Pedrow, P.D., Sablani, S.S., Tang, J., 2023a. Microwave heating based on solid-state generators: new insights into heating pattern, uniformity, and energy absorption in foods. J. Food Eng. 357, 111650.
Zhou, X., Pedrow, P.D., Tang, Z., Bohnet, S., Sablani, S.S., Tang, J., 2023b. Heating performance of microwave ovens powered by magnetron and solid-state generators. Innov. Food Sci. Emerg. Technol. 83, 103240.
Zhou, X., Tang, J., 2024. Microwave-assisted thermal sterilization and pasteurization. In: Pratap Singh, A., Erdogdu, F., Wang, S., Ramaswamy, H.S. (Eds.), Microwave Processing of Foods: Challenges, Advances and Prospects: Microwaves and Food. Springer, pp. 253–272.
Zhou, X., Czekala, P., Olszewska–Placha, M., Salski, B., Zhang, S., Pedrow, P.D., Sablani, S.S., Tang, J., 2024. Understanding microwave heating of oils. J. Food Eng. 375, 112039.